Supporting information

Influence of the substituent in the benzene ring on the structure and properties of two isostructural crystals

Zhonghua Li[a,b], Shengzhe Jia[b,c], Songgu Wu[b,c*], Junbo Gong[b,c]

[a] *Sinopec Research Institute of Petroleum Processing Co., Ltd., Beijing 100083, People's Republic of China*

[b] *State Key Laboratory of Chemical Engineering, School of Chemical Engineering and Technology, Tianjin University, Tianjin 300072, China*

[c] *Haihe Laboratory of Sustainable Chemical Transformations, Tianjin 300192, P. R. China*

1. Experimental section

1.1. Materials

The raw materials of MAMB (purity > 98%) and MAMOB (purity > 99%) were provided by Tianjin Xiensi Opd Technology Co., Ltd and used without further purification. Analytical reagent-grade solvents including hexane, toluene, tetrahydrofuran (THF) and dimethyl sulfoxide (DMSO) were purchased from Shanghai Aladdin Biochemical Technology Co., Ltd.

1.2. Preparation of single crystals with sublimation

The sublimation experiments were carried out for MAMB and MAMOB, respectively. The samples used were both from commercially available powders. The sample was placed in the center of the Petri dish, directly above the heater. The amount of sample added was about 40-50 mg, and the sublimation temperature ranged from 30-35 ℃, which was controlled by the heater. The sublimation time was 5-8 h. Then the crystals sublimed onto the glass plate above the petri dish were observed the crystal morphology with an optical microscope, and single crystals with high quality were selected for single-crystal X-ray diffraction characterization to achieve the crystal structure determination.

1.3. Powder X-ray diffraction (PXRD)

PXRD was performed on D/MAX-2500 X-ray diffractometer (Rigaku, Japan) using Cu Kα radiation (λ = 1.54178 Å). The operating voltage and current of the generator were set to 40 kV and 100 mA, respectively. Samples were measured in the 2θ range of 2−40° at a scan rate of 10°/min. All the PXRD data were acquired at ambient temperature and analyzed with Jade 6.0 software.

1.4. Single-Crystal X-ray diffraction (SCXRD)

SCXRD measurements were performed with Rigaku 007HF XtaLAB P200 diffractometer using Mo Kα radiation (λ = 0.71073 Å) with a graphite monochromator. Suitable single crystals of MAMB and MAMOB were selected and set on a ROD, Synergy Custom system, HyPix diffractometer, separately. Data collection was carried out at 113.15 K. Olex2 [1] was used to solve the crystal structures by intrinsic phasing methods (ShelXT). The model refinement was

conducted by the full-matrix least-squares technique with SHELXL [2]. Mercury [3] software was used for the simulation of PXRD patterns and crystal structure analysis. The crystallographic data has been deposited with Cambridge Crystallographic Data Centre (CCDC), and signed to CCDC code 2216575 for MAMB, 2216574 for MAMOB.

1.5. Optical characterizations

The absorption spectra were recorded with UV-vis spectroscope (Hach, DR3900, USA). The emission spectra, and fluorescence lifetimes of MAMB and MAMOB crystal samples were recorded with an Edinburgh instrument (FLS1000, UK). The quantum yields were measured using an integrating sphere on an Edinburgh FLS1000 spectrometer.

1.6. Computational methods

1.6.1. Hirshfeld surface and 2D fingerprint plots analysis

Hirshfeld surface analysis (HS) analysis [4] and 2D fingerprint plots were generated with CrystalExplorer 17.5 software for visually investigating and quantitatively characterizing the intermolecular interactions in different crystal structures. The red-white-blue coloring scheme corresponds to contacts shorter, equal, and longer than the sum of the van der Waals radii, respectively.

1.6.2. Packing similarity analysis

The structural similarities between MAMB and MAMOB were investigated with XPac [5] program. This method helps to identify the supramolecular construct and the extent of crystal packing dissimilarity between two crystal structures. When executing the program, the filtering parameters were set to default values, where the angular deviation Δa was set to 10°, the interplanar angular deviation Δp was set to 14°, and the corresponding deviation of molecular centroid distance D was set to 0.

1.6.3. Frontier molecular orbital

Geometry optimizations were performed using the B3LYP/lanl2dz level of theory with Gaussian 16 [6] software package. The frontier molecular orbital calculations were conducted based on M06-2X/def2-TZVP level of theory and represented by VMD 1.9.2 software.

2. Tables and Figures

Table S1. Hydrogen bonds in crystal structures of MAMB and MAMOB.

	D-H···A	d(D-H), Å	d(H···A), Å	d(D-A), Å	∠(DHA), deg.	symmetric code
MAMB	N_1-H_{1A}···O_1	0.873	2.130	2.968	160.62	[-x+y+1/3, -x+2/3, z+2/3]
	N_1-H_{1B}···O_1	0.874	2.047	2.694	130.17	
	C_3-H_3···O_1	0.950	2.572	3.343	138.46	[-x+y+1/3, -x+2/3, z+2/3]
MAMOB	N_1-H_{1A}···O_1	0.867	2.224	3.049	158.96	[-x+y+1/3, -x+5/3, z+2/3]
	N_1-H_{1B}···O_1	0.894	2.064	2.715	128.79	
	C_3-H_3···O_1	0.950	2.597	3.364	138.03	[-x+y+1/3, -x+5/3, z+2/3]

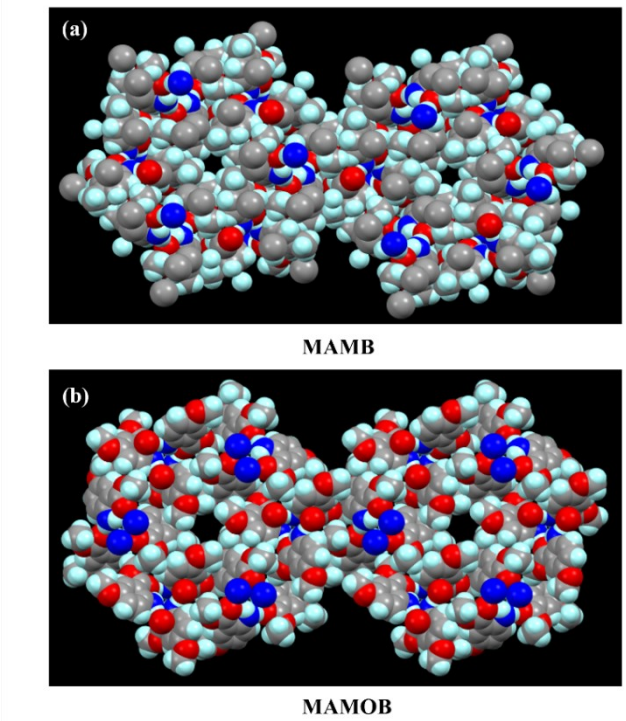

Fig. S1. Comparison of packing patterns in *ab* plane for isostructural crystals MAMB and MAMOB.

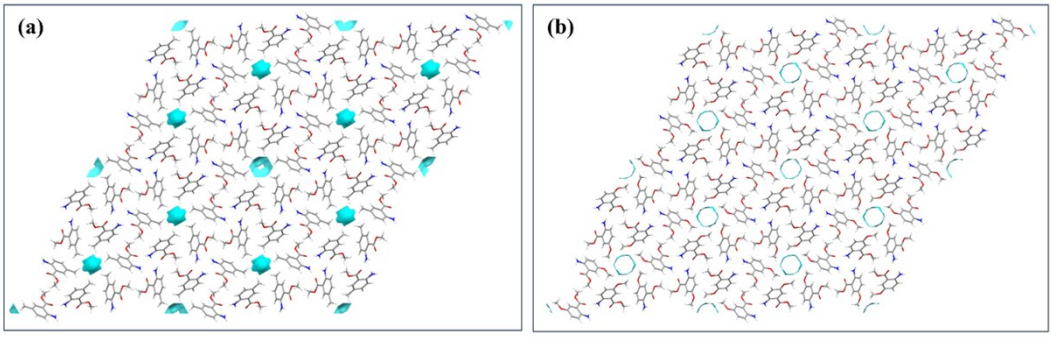

Fig. S2. Packing view of MAMB and MAMOB crystals in *ab* plane.

Table S2. The detailed photophysical data for the obtained polymorphs of MAMB and MAMOB.

Name	Voids volume	Voids percentage
MAMB	71.94 Å^3	1.8%
MAMOB	150.54 Å^3	3.7%

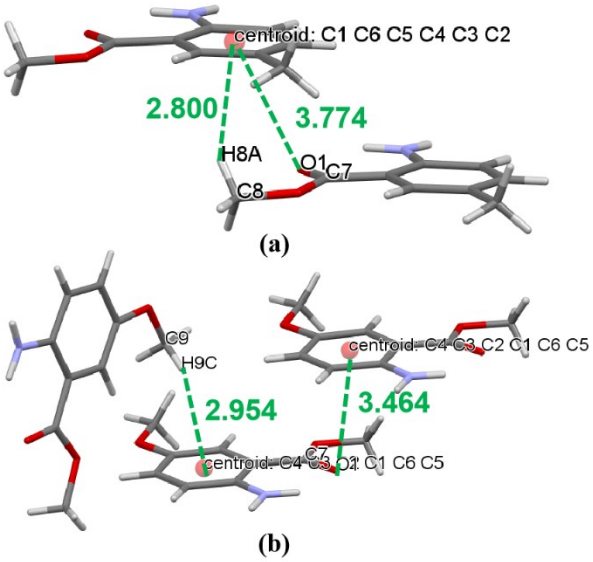

Fig. S3. (a) C–H···π and C=O···π intermolecular interactions in MAMB, (b) C–H···π and C=O···π intermolecular interactions in MAMOB.

Table S3. The Geometric details of the C–H···π and C=O···π intermolecular interactions.

Name	Intermolecular interaction	H, O···π (A˚)	C···π (A˚)	Angle (°)	Symmetry operator
MAMB	C_8-H_{8A}···π	2.800	3.660	147	x, y, -1+z
MAMB	$C_{7=}O_1$···π	3.774	3.902	86.88(11)	x, y, -1+z
MAMOB	C_9-H_{9c}···π	2.954	3.656	129	-1/3+y, 1/3-x+y, 4/3-z
MAMOB	$C_{7=}O_1$···π	3.464	3.650	88.89(10)	x, y, -1+z

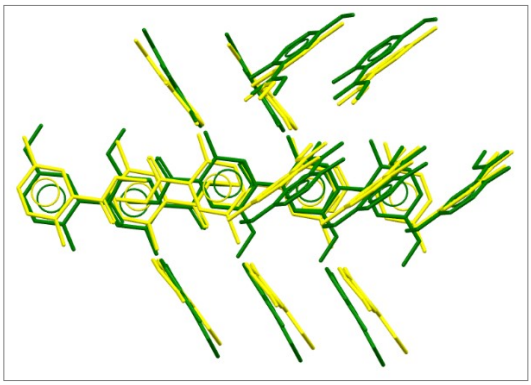

Fig. S4. Comparison of packing similarity of MAMB (marked yellow) and MAMOB (marked green) with Mercury software.

Table S4. The detailed photophysical data for MAMB and MAMOB.

Name	$\lambda_{max,em}$ (nm)	B_1	τ_1 （ns）	B_2	τ_2 （ns）	τ_{av} （ns）	Φ_F (%)
MAMB	424	853.0619	2.4002	2086.0112	8.0091	7.40	54.93
MAMOB	439	1211.6852	1.5611	1998.4257	4.0669	3.59	10.52

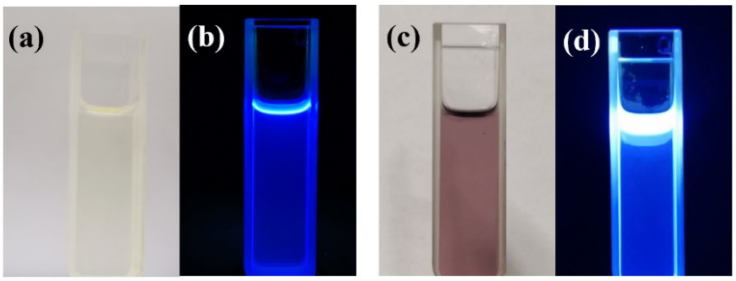

Fig. S5. (a, b) Daylight and fluorescence photographs of MAMB in dichloromethane solvent, and (c, d) daylight and fluorescence photographs of MAMB in dichloromethane solvent.

References

[1] O. V. Dolomanov, L. J. Bourhis, R. J. Gildea, *J. Appl. Crystallogr.*, 2009, **42**, 339-341.

[2] G. Sheldrick, G. M. Sheldrick, G. M. Sheldrick, SHELXL-97. Program for the Refinement of Crystal Structures, 1997.

[3] C. F. Macrae, P. R. Edgington, P. McCabe, E. Pidcock, G. P. Shields, R. Taylor and J. V. D. Streek, *J. Appl. Crystallogr.*, 2006, **39**, 453-457.

[4] M. A. Spackman and D. Jayatilaka, *CrystEngComm*, 2009, **11**, 19-32.

[5] T. Gelbrich, T. L. Threlfall and M. B. Hursthouse, *CrystEngComm*, 2012, **14**, 5454-5464.

[6] M. Frisch, G. Trucks and H. Schlegel, Gaussian 16. Gaussian, Inc. Wallingford, CT, 2016.